

Article

Impact of Xiaolangdi Reservoir on the Evolution of Water Infiltration Influence Zones of the Secondary Perched Reach of the Lower Yellow River

Min Zhang ^{1,2} , Jianhua Ping ^{2,3,*}, Yafei Zou ^{2,3}, He Li ^{1,2} , Joshua Mahwa ^{1,2,4} , Jichang Zhao ⁵ and Jiaqi Liu ^{2,3}

- ¹ College of Water Conservancy and Transportation, Zhengzhou University, Zhengzhou 450001, China; minzhang927@163.com (M.Z.); lh13837110114@163.com (H.L.); mahwajoshua@yahoo.com (J.M.)
- ² Geothermal and Ecological Geology Research Center, Zhengzhou University, Zhengzhou 450001, China; zouyafei@zzu.edu.cn (Y.Z.); liujq@mail.iggcas.ac.cn (J.L.)
- ³ College of Ecology and Environment, Zhengzhou University, Zhengzhou 450001, China
- ⁴ Department of Geology, College of Earth Science and Engineering, University of Dodoma, Dodoma P.O. Box 11090, Tanzania
- ⁵ China Institute of Geo-Environmental Monitoring, Beijing 100081, China; jichzhao@163.com
- * Correspondence: pingjianhua@zzu.edu.cn

Abstract: Understanding the complex interplay between water management infrastructure and groundwater dynamics is crucial for sustainable resource utilization. This study investigates water infiltration dynamics in the secondary perched reach of the Yellow River after the operation of the Xiaolangdi Reservoir. The methodology included the application of the single-factor analysis of variance and water balance method, alongside a dual-structure, one-dimensional seepage model to simulate interactions within the system, while exploring characteristics of the groundwater flow system and the exploitation depth of below 100 m. Furthermore, we studied the influence zone range and alterations in river water infiltration in the secondary perched reach of the river following the operation of Xiaolangdi Reservoir. The results show that before the operation of the reservoir, the influence ranges of the north and south banks of the aboveground reach extended from 20.13 km to 20.48 km and 15.85 km to 16.13 km, respectively. Following the initiation of the reservoir, the river channel underwent scouring, leading to enhanced riverbed permeability. Additionally, the influence of long-term groundwater exploitation on both riverbanks extended the influence range of groundwater recharge within the secondary perched reach of the river. The influence zone of the north bank is now 23.41 km–26.74 km and the south bank 18.43 km–21.05 km. After years of shallow groundwater extraction, multiple groundwater depression cones emerged within the five major groundwater source areas on both sides of the river. Notably, deeper water levels (Zhengzhou to Kaifeng) have significantly decreased, with a drop of 42 m to 20 m to 15 m. This change in groundwater dynamics extended beyond the main channel of the river, creating a localized shallow groundwater field.

Keywords: Xiaolangdi Reservoir; the Yellow River; secondary perched river; influence zones range; groundwater



Citation: Zhang, M.; Ping, J.; Zou, Y.; Li, H.; Mahwa, J.; Zhao, J.; Liu, J. Impact of Xiaolangdi Reservoir on the Evolution of Water Infiltration Influence Zones of the Secondary Perched Reach of the Lower Yellow River. *Water* **2023**, *15*, 4308. <https://doi.org/10.3390/w15244308>

Academic Editor: Roohollah Noori

Received: 27 October 2023

Revised: 14 December 2023

Accepted: 15 December 2023

Published: 18 December 2023



Copyright: © 2023 by the authors. Licensee MDPI, Basel, Switzerland. This article is an open access article distributed under the terms and conditions of the Creative Commons Attribution (CC BY) license (<https://creativecommons.org/licenses/by/4.0/>).

1. Introduction

The water level of the Yellow River typically stands 5–10 m higher than the groundwater level along both banks, extending approximately 1 km inland [1]. This river water continuously infiltrates aquifers, replenishing the groundwater [2–4]. The extent of the Yellow River's influence zone is determined by the permeability of aquifers, affecting various aspects of the groundwater system, including width, depth, water quantity, and quality [5,6]. The Xiaolangdi Hydraulic Project is located at the outlet of the last canyon section in the middle stretch of the Yellow River. Since the commencement of water and

sediment transfer by the Xiaolangdi Reservoir in July 2002, significant scouring has occurred in the lower reaches of the river [7,8], causing the riverbed to narrow and deepen [9]. Meanwhile, the discharge and water levels have decreased, leading to a drop in the base level of groundwater recharge [4,10–12]. This in turn has altered the shallow groundwater level on both sides of the river as well as in its influence zones.

The lower reaches of the Yellow River contain vast tidal lands, and the abundant groundwater on both sides of the river is an important resource for ensuring the economic activities, livelihoods, and ecological well-being of the local population [10]. Studying the variation in the groundwater recharge zone within the secondary perched reach of the Yellow River before and after the operation of the Xiaolangdi Reservoir holds significant theoretical and practical importance [13,14].

Research on the infiltration influence zone of the secondary perched reach of the Yellow River has been conducted mainly since 2000 [15]. Researchers have carried out a number of studies on river runoff, seepage, and groundwater in typical secondary perched reaches of the lower Yellow River [16–19].

The groundwater dynamics method was used to determine the permeability coefficient of riverbed sediments in the field and to calculate the infiltration range of groundwater charged by river water in the lower Yellow River [20,21]. Furthermore, the interaction between surface water and groundwater, along with its hydrochemical evolution in the secondary perched Yellow River, has been extensively studied based on various factors such as physical geography, geological and hydrogeological conditions, environmental isotopes, and groundwater hydration groups [22–24]. Additionally, a number of researchers have investigated the range of influence of the secondary perched reach infiltration during the early years of formal water and sediment regulation operations of the Xiaolangdi Reservoir [14,25,26].

Previous studies have primarily focused on the infiltration and dynamic characteristics of the groundwater system in the affected zone of the secondary perched reach of the lower Yellow River. However, few studies concentrated on the impact of the long-term operation of reservoirs on the infiltration and groundwater recharge range in the secondary perched reach of the lower Yellow River. Furthermore, since the reservoir has been operating for more than two decades, the bed of the secondary perched reach of the Yellow River has continuously eroded, leading to significant alterations in the influence zone of the secondary perched reach after the operation of the reservoir.

Thus, in this work, Huayankou–Jiahetan hydrological stations, the typical secondary perched reach of the lower Yellow River, were selected as the study area. Using various methods, such as one-way analysis of variance (ANOVA) and a “binary structure” one-dimensional seepage mathematical model, we focused on the dynamic process of the interaction between river water and groundwater before and after the operation of the reservoir. The findings of this study will contribute to shedding light on the evolution pattern of the groundwater influence zone affected by the Yellow River water recharge. Additionally, it allows for a deeper understanding of water circulation characteristics in the secondary perched reach and enables the scientific development and sustainable utilization of groundwater resources in this region.

2. Study Area

The lower reaches of the Yellow River feature are dominated by an accumulation of river channels. Owing to the high sediment content and strong siltation of the river water, the riverbed of the Yellow River stands 3–5 m higher than the surrounding ground, giving rise to the world’s most famous “secondary perched river” (Figure 1).

Since the late Middle Pleistocene of the Quaternary (Q₂₋₂), a large amount of sediment carried by the upper reaches of the Yellow River was deposited and subsequently re-scoured, resulting in the formation of an extensive alluvial plain, with the river serving as a crucial source for shallow groundwater [23]. The study area focuses on the secondary perched reach of the lower Yellow River, which specifically encompasses the section extending from the Zhengzhou Huayankou Hydrological Station to the Kaifeng Jiahetan Hydrological Station, covering a distance of 105 km. This region is located within the mid-

latitude temperate monsoon climate zone and experiences a typical continental climate. It receives an average annual rainfall of 642.8 mm, with an average annual evaporation of 2097.6 mm and an average relative humidity of 67.8%. During winter months, northwest winds prevail, whereas southeast winds dominate during the summer season.

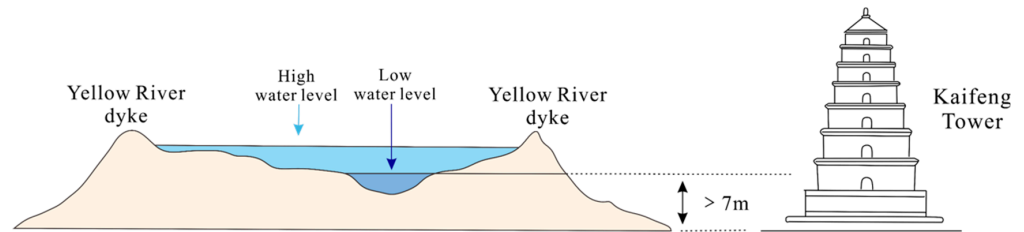


Figure 1. Conceptual map of the secondary perched reach of the Yellow River.

According to regional hydrogeological conditions, it is evident that this area constitutes an aquifer highly susceptible to submersion. The depth of the aquifer’s base generally ranges between 60 and 120 m, with the deepest at 140 m, which is located in northern Kaifeng. Using pertinent data, the study area was divided into eight distinct shallow underground aquifer areas (Figures 2 and 3). The study area was selected based on these lithological characteristics that gave rise to the largest zone for groundwater infiltration and recharge along the lower Yellow River.

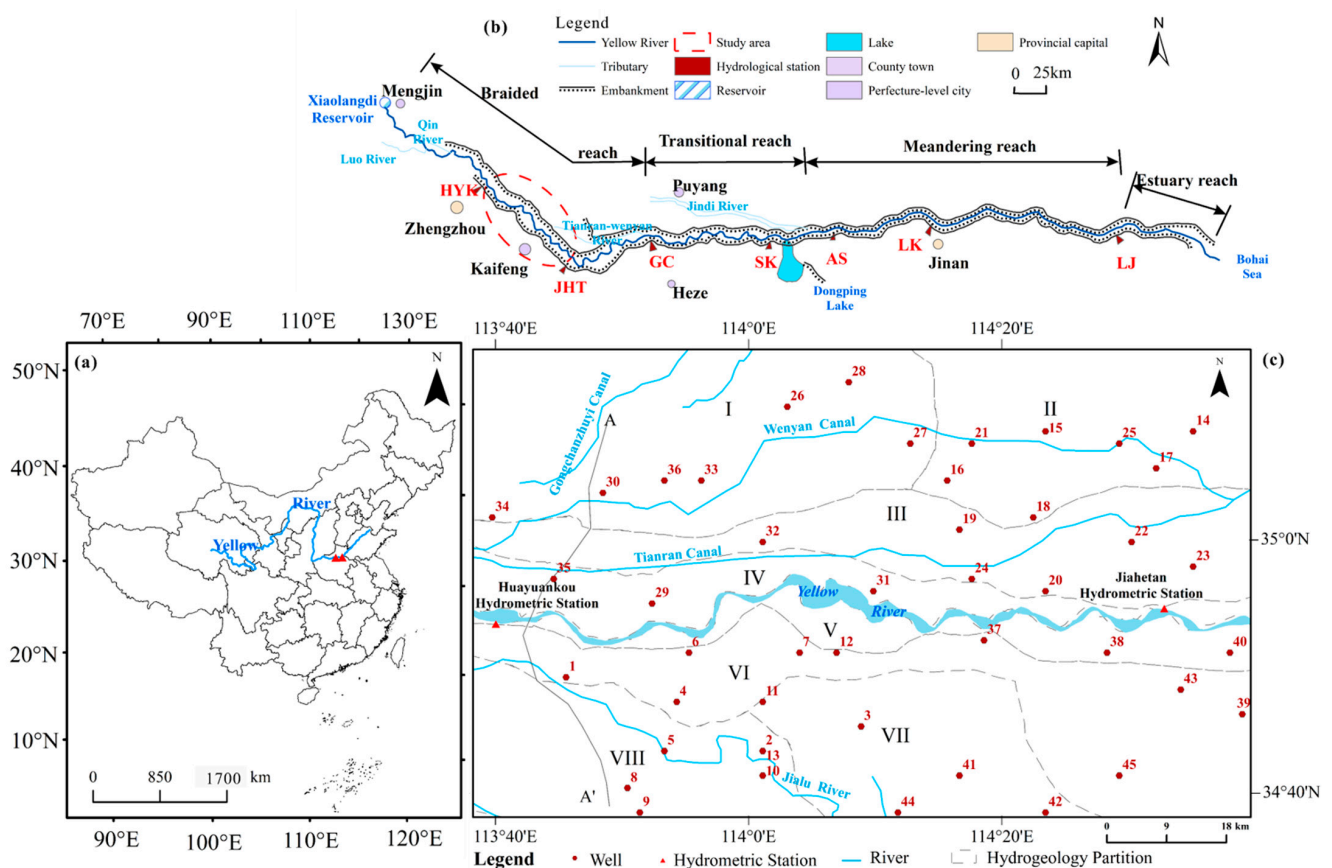


Figure 2. Location and hydrogeological division of the study area. (a) The location of the study area in China. (b) Schematic diagram of the location of the study area in the lower reaches of the Yellow River. Monitoring well location and hydrogeological zoning. Notes: Zone I is located on the north bank of the Yellow River, approximately 12–30 km west of the riverbed, near the eastern foothills of

(c) Taihang Mountain. The aquifer lithology predominantly comprises interbedded sub-sandy soil, silty sand, and fine sand. Zone II is situated on the eastern side of Zone I, approximately 13–26 km from the riverbed. In these regions, the shallow aquifer lithology primarily comprises sub-sandy soil and silty sand interbeds. Region III, located on the northern bank of the river, is a high-flood beach area and features natural channels across the region from west to east. The shallow aquifer lithology in Region III comprises sub-sandy soil and silty sand interbeds. In contrast, the aquifer in Region IV primarily consists of sub-sandy soil. Region V represents a flooded beach area on the southern bank of the Yellow River, characterized by aquifer lithology primarily composed of sub-sandy soil or silty sand with well-developed pores that enhance atmospheric precipitation infiltration and recharge. The aquifer lithology of Region VI is predominantly sub-sandy soil, whereas that of Region VII mainly consists of silty fine sand. The aquifer lithology of Region VIII comprises dunes, sub-sandy soil, and silty sand.

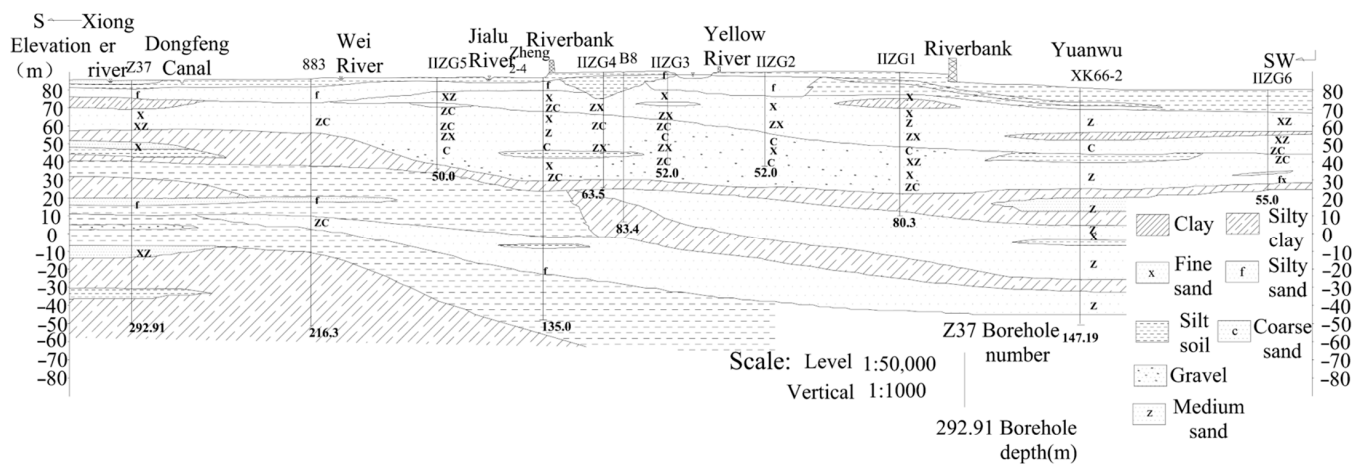


Figure 3. Hydrogeological profile of the study area

3. Materials and Methods

3.1. Materials

The groundwater data used in this study were obtained from various reliable sources, with the Henan Provincial Bureau of Hydrology and Water Resources serving as the primary data source, with a focus on annual groundwater level data from 1980 to 2017 (Table 1).

Table 1. Annual average groundwater level of representative monitoring wells along the Yellow River (m).

Well	Year									
	1980	1985	1990	1995	2000	2005	2010	2015	2017	
6	81.94	82.69	82.65	80.63	81.46	81.50	80.43	78.33	77.16	
7	78.10	79.18	79.37	79.15	79.07	77.74	77.22	74.18	72.96	
12	77.54	79.18	78.00	77.92	77.23	78.27	77.62	74.65	74.60	
20	72.03	72.55	71.81	71.80	71.39	71.56	71.12	69.42	67.97	
23	65.33	65.92	64.44	65.35	64.99	65.07	65.07	63.98	63.08	
24	72.19	73.62	72.20	72.49	71.55	71.77	71.70	68.96	69.02	
29	85.46	85.82	86.08	84.91	84.92	84.85	80.01	79.23	81.55	
31	78.87	78.91	78.48	79.09	78.55	77.62	76.36	76.03	76.52	
32	76.71	76.86	78.10	77.72	77.98	78.00	76.66	75.84	76.07	
37	76.18	75.93	76.73	76.58	76.30	75.81	75.40	74.82	74.46	
38	71.86	72.41	71.19	72.42	70.71	70.19	70.83	69.59	68.97	
40	67.87	67.61	67.39	67.56	66.81	66.92	66.16	63.97	64.89	

Additionally, the Huayuankou Hydrological Station on the Yellow River contributed data, including water level, flow, and water diversion statistics, which were accessed

through the monitoring platform managed by the Ministry of Water Resources of the Yellow River Conservancy Commission. The groundwater extraction data were obtained from the Zhengzhou Water Resources Bulletin, the Xinxiang Water Resources Bulletin, and the Kaifeng Water Resources Bulletin, compiled by their respective Water Resources Bureaus.

3.2. Methods

This study employed a methodology that analyzed the correlation between the water levels in the lower reaches and well points using a linear correlation analysis. We used meteorological, hydrological, and groundwater monitoring data from 1980 to 2017 for the study area, both before and after the operation of the Xiaolangdi Reservoir. The principles of groundwater dynamics and a one-dimensional seepage model of “dual structure” were applied to calculate and analyze the influence zone width of the secondary perched reach before and after the operation of the reservoir [14,27]. Additionally, the hydraulic slope $J = \Delta h/L$ of the groundwater level in the secondary perched reach and in the wells was calculated based on the infiltration influence distance of the secondary perched reach and the hydrogeological conditions of the study area [13]. The change in the recharge of the secondary perched reach river to the groundwater was then calculated by analyzing the variation in hydraulic slope using IBM SPSS Statistics 26.0.0.0 software and conducting a one-way ANOVA [28,29].

3.2.1. One-Way Analysis of Variance

One-way ANOVA is a statistical method that calculates the effect of a subtype independent variable on a numerical independent variable. Depending on the context, several key components are considered, including the null hypothesis, the test statistic F , and the interpretation of observed values and p -values.

- (i) Null hypothesis: The null hypothesis for one-way ANOVA, denoted as H_0 , posits that there is no significant difference between the mean values of observed variables at different levels of control variables. This implies that X_{ij} , representing an individual data point in the dataset, can be considered as originating from the same unified population, expressed as $H_0: \mu_1 = \mu_2 = \dots = \mu_k$, where μ represents the population of each group.
- (ii) Statistic F is selected as the test statistic to determine its distribution, using the following equation:

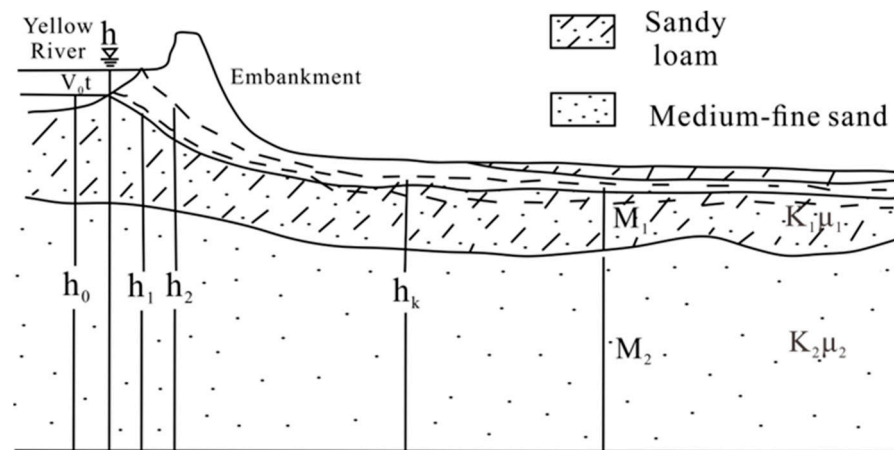
$$F = \frac{SSA/(k-1)}{SSE/(n-k)} = \frac{MSA}{MSE}$$

where SSA is the sum of squares between groups; SSE is the sum of squares within groups; k is the number of independent variable groups; n is the total number of data points; MSA is the mean square of the variation between groups; and MSE is the mean square of the variation within each group.

- (iii) The observed and probability p -values of the test statistics are calculated. If the control variable significantly impacts the observed variable, compared to the random variable, the proportion of the control variable in the total variation of the observed variable should be larger, resulting in an F -value greater than 1. Conversely, if the control variable has little influence on the observed variable, then the variation in the observed variable should be primarily attributed to the influence of the random variable, and the F -value should be approximately equal to 1.

3.2.2. “Dual Structure” One-Dimensional Seepage Mathematical Model

Groundwater recharge through runoff infiltration and infiltration during unsteady flow conditions generally remains constant or experiences minimal changes, while percolation becomes more prominent during steady flow conditions. Figure 4 illustrates the complete process of one-dimensional infiltration. The mathematical model for this “binary-structure” one-dimensional flow is expressed by the following mathematical equations [30–32]:



- h - high water level of Yellow River (m)
- V_0t - a variation of water level of Yellow River, $h-h_0$
- h_0 - Yellow River low water level (m)
- h_1 - groundwater level at a low water level of Yellow River (m)
- h_2 - groundwater level at a high water level of Yellow River (m)
- h_k - water table at a certain distance from the Yellow River (m)
- M_1, M_2 - weak aquifer, aquifer thickness (m)
- K_1, μ_1 - permeability coefficient and water storage coefficient of aquifer
- K_2, μ_2 - permeability coefficient and water storage coefficient of weak aquifer

Figure 4. Schematic diagram of the one-dimensional infiltration unit.

Aquitard

$$\mu_1 \frac{\partial h_1}{\partial t} = \frac{K_1}{M_1} (h_2 - h_1) \tag{1}$$

where μ_1 represents specific yield; h_1 and h_2 represent the low and high groundwater levels of the Yellow River, respectively (m); t is the time (day); $\frac{K_1}{M_1} = \epsilon$, ϵ is a calculation parameter with K_1 being the permeability coefficient (m/day); and M_1 is the aquifer thickness (m).

Micro confined aquifer

$$T_2 \frac{\partial^2 h_2}{\partial x_2^2} - \epsilon (h_2 - h_1) = \mu_2 \frac{\partial h_2}{\partial t} \tag{2}$$

where $T_2 = K_2 M_2$ is the water conductivity coefficient (m^2/d); h_1 and h_2 are the groundwater levels at low- and high-water levels of the Yellow River, respectively (m); x_2 is the infiltration distance (m); ϵ is a calculation parameter; μ_2 is the storage coefficient; and t is the time (day).

When a significant amount of time has elapsed, specifically when $t > (20/\eta) \times (M_1^2/a_1)$, Equation (2) can be expressed as follows:

$$(h_2 - h_1)_{x,t} = V_0 t \cdot 4i^2 \operatorname{erfc} \left(\frac{X}{2\sqrt{at}} \right) \tag{3}$$

$$a = \frac{T_2}{\mu_1 + \mu_2} \tag{4}$$

where t represents the time required for the water level to transition from its lowest to its highest point; η represents a calculation parameter associated with 'binary structure'; M_1 refers to the thickness of the weak aquifer (m); a_1 represents the conductance coefficient (m^2/d); $(h_2 - h_1)$ indicates the change in groundwater level during time t ; x represents the range of influence; V_0 represents the change rate of the water level of the Yellow

River (whether rising or falling); $4i^2 \operatorname{erfc}\left(\frac{X}{2\sqrt{at}}\right)$ represents the influence coefficient; a represents the conductance coefficient (m^2/d); T_2 refers to the hydraulic conductivity coefficient of a micro-confined aquifer; μ_1 denotes the weak aquifer water supply; and μ_2 denotes the water release coefficient of a micro-confined aquifer.

For a given change in the Yellow River water level (V_0t), a corresponding change occurs in the water table (Δh). When the groundwater level change is 5%, that is, $V_0t \cdot 4i^2 \operatorname{erfc}\left(\frac{X}{2\sqrt{at}}\right) = 5\%$, this point is considered the critical point of the sweep. The distance from this critical point to the shoreline is defined as the sweep range (X) [33]. Specific values can be obtained using the following equation, which shows that as the duration of time (t) increases, the influence range (X) also extends further:

$$X = 3.216\sqrt{at} \quad (5)$$

where X represents the width of the Yellow River groundwater recharge (m); a denotes the conductance coefficient (m^2/d); and t represents the time it takes for the water level of the Yellow River to transition from its lowest to its highest value (d).

4. Results

4.1. Relationship between Secondary Perched River Water and Groundwater

4.1.1. Division of Hydrological Runoff into Wet, Normal, and Dry Years

In the study, we used the anomaly percentage P as defined in the standard for hydrological information and hydrological forecasting (GB/T22482-2008) [34] as the standard for classifying the runoff as either high or flat in the Huayuankou–Jiahetan secondary perch reach. The years between 1980 and 2017 were categorized into periods of high, flat, and low runoff, based on the anomaly percentage formula:

$$P = (\text{annual runoff} - \text{annual average runoff}) / \text{annual average runoff} \times 100\%$$

These periods were further classified as wet, normal, and dry years. According to the classification criteria of wet, normal, and dry years, the runoff was divided into four distinct periods: 1980–1994 was categorized as the wet year period, 1995–2002 was the dry year period, 2003–2011 was the normal year period, and 2012–2017 was another dry year period (Figure 5).

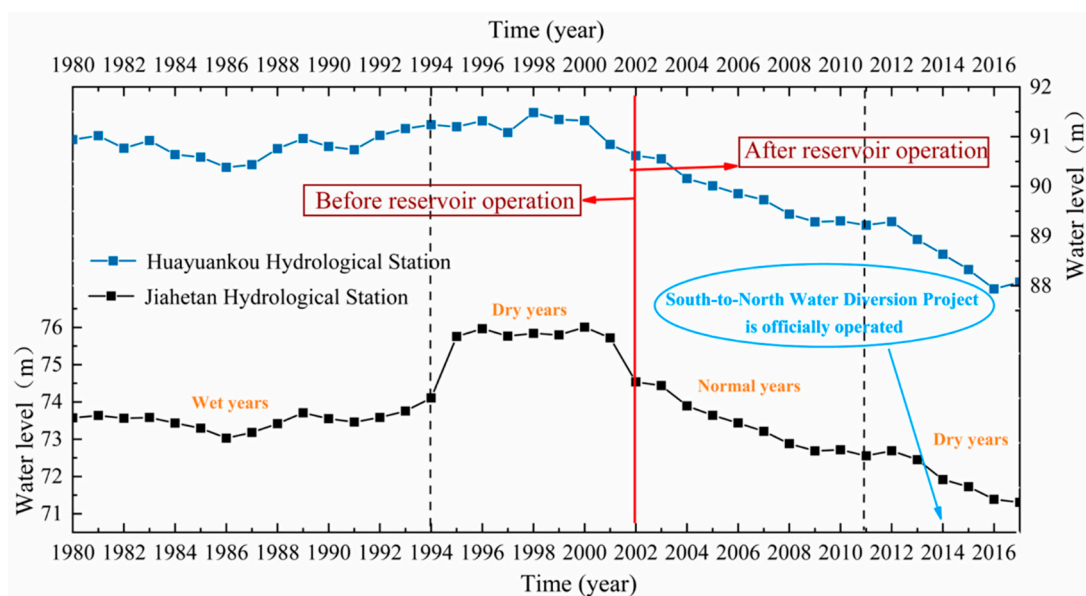


Figure 5. Changes in river water level at two hydrological stations.

4.1.2. Fluctuations in Water Levels at the Huayuankou and Jiahetan Hydrological Stations

The Huayuankou and Jiahetan hydrological stations exhibited a clear trend of gradually declining water levels over the past four decades. Specifically, the water level at the Huayuankou Hydrology Station decreased by 3.54 m, while that at the Jiahetan Hydrological Station decreased by 4.7 m. In 1998, before the operation of the Xiaolangdi Reservoir, the highest water level recorded at the Huayuankou Hydrological Station was 91.48 m. However, after the reservoir was built, the lowest water level recorded was 87.94 m in 2016, indicating a difference of 3.55 m. Similarly, before the reservoir's operation, the highest water level recorded at the Jiahetan Hydrological Station was 76.01 m in 2000. However, the river level has continuously decreased since the reservoir began operation in 2002, reaching its lowest water level of 71.31 m in 2017 (Figure 5). After years of water quantity and water level monitoring, it has become evident that external factors, such as the Yellow River diversion project and riverside water sources, exert a more pronounced influence on the river water level at the Jiahetan Hydrological Station compared with the Huayuankou Hydrological Station.

Before the operation of the Xiaolangdi Reservoir, the variation in the water level in the secondary perched reach river was relatively small during the wet years from 1980 to 1994 and in the dry years from 1995 to 2002, with a gradual upward trend. However, after the reservoir's operation in 2002, the water level of the reservoir in both normal years (from 2003 to 2011) and dry years (from 2012 to 2017) exhibited more significant fluctuations and an obvious downward trend.

4.1.3. Relationship between Surface Water and Groundwater Levels in the Secondary Perched Reach of the Yellow River

Based on monitoring data over many years, the correlation between river water and groundwater in the secondary perched reach of the Yellow River was analyzed both before and after reservoir operation. Our findings indicated the following: (1) Before the reservoir operation, approximately 73% of the correlation coefficients were negative, with only 27% being positive. The highest correlation values were observed in wells #26, #31, and #32, which are located on the north bank of the Yellow River, near the midpart of the two hydrological stations (Figure 2). (2) After the reservoir operation, all correlation coefficients became positive, with the highest values observed in wells #7, #27, #36, #35, #26, and #21. Notably, well #7 is located on the northern bank, while most of the wells are closer to the Huayuankou Hydrological Station (Figure 6, Table 2).

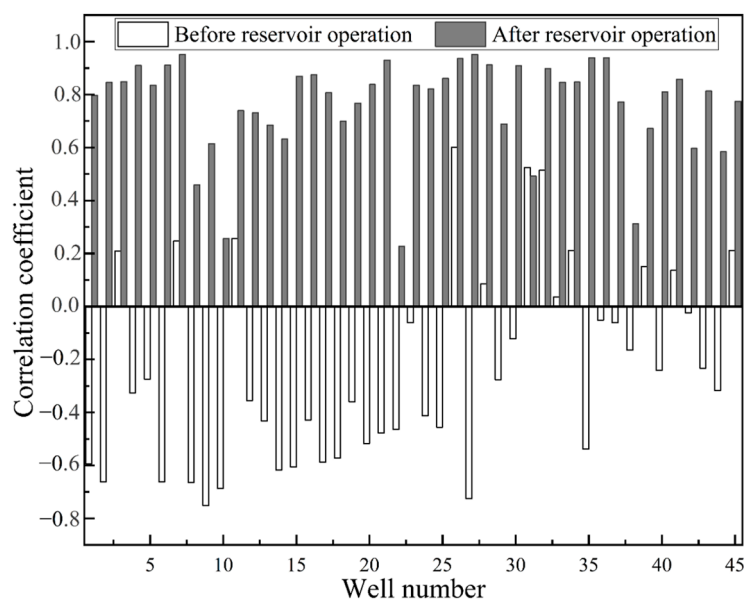


Figure 6. Correlation between surface water and groundwater levels.

Table 2. Correlation coefficient between river water and groundwater levels.

Wells	Correlation Coefficient		Wells	Correlation Coefficient		Wells	Correlation Coefficient	
	Before Reservoir Operation	After Reservoir Operation		Before Reservoir Operation	After Reservoir Operation		Before Reservoir Operation	After Reservoir Operation
1	−0.594	0.797	16	−0.429	0.875	31	0.525	0.492
2	−0.662	0.846	17	−0.588	0.807	32	0.514	0.898
3	0.210	0.849	18	−0.572	0.699	33	0.036	0.846
4	−0.326	0.910	19	−0.359	0.767	34	0.212	0.847
5	−0.274	0.835	20	−0.517	0.838	35	−0.538	0.939
6	−0.662	0.911	21	−0.478	0.930	36	−0.051	0.939
7	0.247	0.951	22	−0.464	0.228	37	−0.062	0.772
8	−0.664	0.460	23	−0.062	0.835	38	−0.165	0.312
9	−0.751	0.614	24	−0.413	0.821	39	0.151	0.672
10	−0.687	0.257	25	−0.456	0.861	40	−0.241	0.810
11	0.257	0.739	26	0.601	0.936	41	0.136	0.858
12	−0.355	0.732	27	−0.725	0.951	42	−0.024	0.597
13	−0.432	0.685	28	0.086	0.912	43	−0.233	0.813
14	−0.618	0.633	29	−0.276	0.688	44	−0.317	0.584
15	−0.606	0.869	30	−0.122	0.909	45	0.212	0.774

In summary, after the operation of the Xiaolangdi Reservoir, the correlation between the groundwater level and the water level of the Yellow River increased significantly and became strongly positive, indicating that the groundwater level increased with an increase in the water level of the river. This phenomenon may be attributed to the reservoir's regulation and storage, which prevented the lower reaches of the Yellow River from becoming isolated. Consequently, the river water continued to infiltrate the aquifer, strengthening the correlation with groundwater [24]. Simultaneously, the wells on the north bank of the river exhibited a stronger correlation. This may be because the north bank primarily encompasses the mainstream zone of the ancient river channel, which is characterized by coarser particles, compared with the south bank. The lithologies of hydrogeological zones I, II, III, and IV on the north bank include interbedded fine sand and sandy soil, with a high permeability coefficient. In contrast, zones V, VI, VII, and VIII on the south bank consist of interbedded fine sand and clay, leading to a thicker, weak aquifer and relatively weaker contribution of the river to groundwater in these areas.

4.2. Infiltration Process and Influence Zone of the Secondary Perched Reach of the Yellow River

4.2.1. Conceptual Model of the Groundwater Dynamic Field

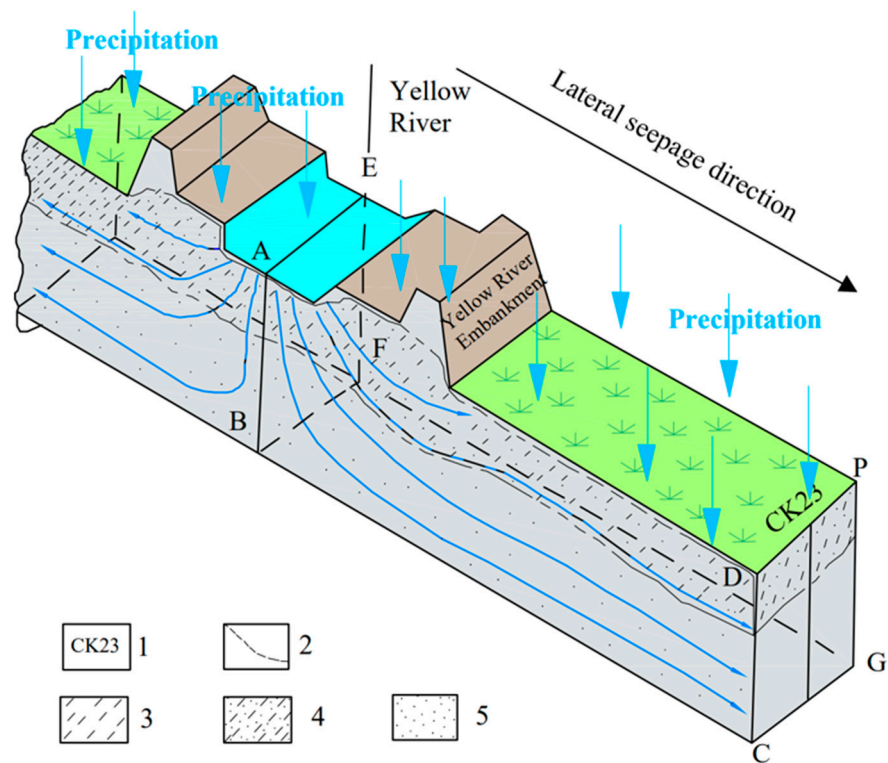
(1) “Dual-structure” one-dimensional infiltration model

Using the “dual-structure” one-dimensional infiltration mathematical model [35] in conjunction with eight hydrogeological zones, the influence zones of the secondary perched reach of the Yellow River were determined across the four hydrological periods. The guiding pressure coefficient on the south bank of the secondary perched reach of the Yellow River was $285\ 714.29\ \text{m}^2/\text{d}$, while on the north bank, it was $463\ 750\ \text{m}^2/\text{d}$. During the wet period from 1980 to 1994, the time taken for the water level of the secondary perched reach of the river to change from its lowest to highest value was 85 days. However, during the dry period from 1995 to 2002, this annual time extended to 88 days. The normal period from 2003 to 2011 had a duration of 115 days, whereas the low-water-level period from 2012 to 2017 lasted 150 days. By substituting the aforementioned durations and conduction coefficients into Equation (5), the influence ranges of the secondary perched reach on the north and south banks of the Yellow River during 1980–1994 were 20.13 km and 15.85 km, respectively. From 1995 to 2002, the influence range on the northern riverbank was 20.48 km, whereas that on the southern riverbank reached 16.13 km. During 2003–2011, the influence range on the northern riverbank further increased to 23.41 km, while that on the southern riverbank reached 18.43 km. From 2012 to 2017, the influence range on the northern riverbank expanded to 26.74 km, and that on the southern riverbank covered a distance of 21.05 km (Table 3, Figure 7). Meanwhile, Table 3 shows that before the operation of the Xiaolangdi Reservoir, the required duration to transition from the lowest to the highest water level and the influence distance remained relatively stable. After the operation of

Xiaolangdi Reservoir, due to the impact of changes in river flow, river level, river bottom penetration strength, and riverside groundwater level, the number of days from the lowest water level to the highest water level increased and the affected distance increased, but they did not increase in the same proportion. In addition, this analysis considers the influences of increasing river runoff, decreasing river level, and potential errors in the average pressure conductivity coefficient. Therefore, the influence distance and range of the Yellow River water recharge to groundwater should be determined based on the actual monitoring data from the monitoring wells.

Table 3. ‘Dual-structure’ one-dimensional infiltration mathematical model to calculate the Yellow River water infiltration recharge groundwater influence zone.

Periods	Location	Time to Change from the Lowest to Highest Water Level (days)	Conductivity Factor (m ² /d)	Influence Distance (km)
1980–1994	southern bank	85	285,714.29	15.85
	northern bank		463,750.0	20.13
1995–2002	southern bank	88	285,714.29	16.13
	northern bank		463,750.0	20.48
2003–2011	southern bank	115	285,714.29	18.43
	northern bank		463,750.0	23.41
2012–2017	southern bank	150	285,714.29	21.05
	northern bank		463,750.0	26.47



1. Drilling; 2. groundwater level; 3. mild clay; 4. sandy loam; 5. medium-fine sand. BC: Seepage width; AE: the recharge boundary of the Yellow River as a recharge source; AEPD: upper boundary of the aquifer; BFCG: aquifer floor elevation

Figure 7. ‘Dual-structure’ one-dimensional infiltration model

(2) Characteristics of the groundwater dynamic field

In the lower plains of the Yellow River, the shallow groundwater follows a radial flow pattern with the river as its central axis, moving towards the southeast and northeast.

However, along the riverbank zone that is affected by the infiltration and recharge from the secondary perched reach of the Yellow River, the groundwater flow direction is almost perpendicular to that of the river. This distinction serves as the basis for the division of the influence zone of the river. Based on characteristics of groundwater flow, during the period 1980 to 1994, the influence zone on the north bank extended approximately 18 km, while that on the south bank covered approximately 14 km (Figure 8). However, from 2012 to 2017, the influence zone on the northern riverbank expanded by approximately 27 km, whereas the influence zone on the southern riverbank reached approximately 22 km (Figure 9).

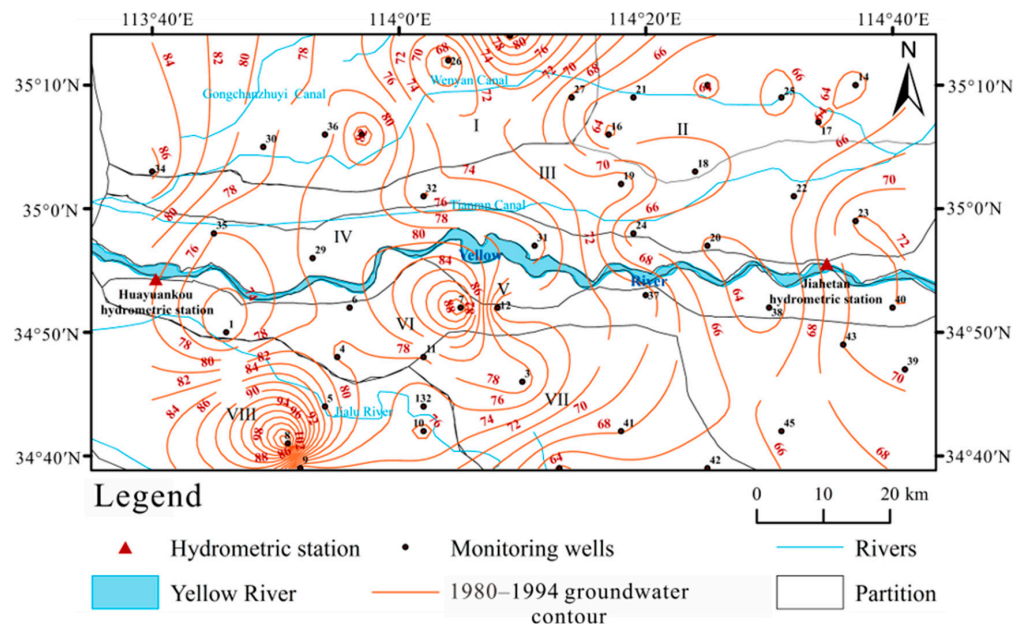


Figure 8. Influence range of seepage recharge groundwater from 1980 to 1994.

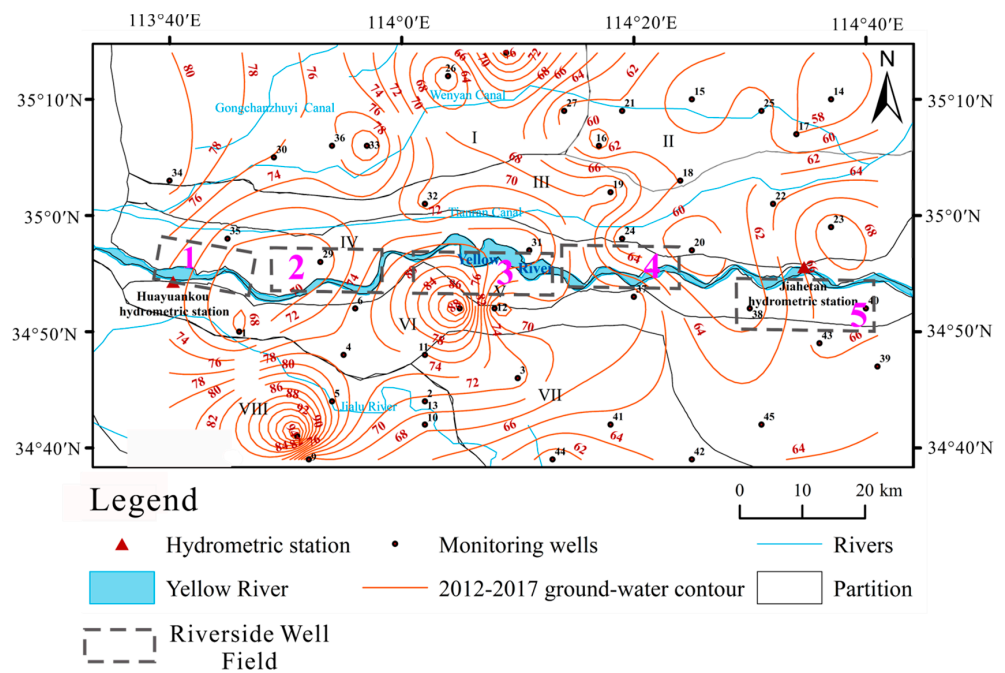


Figure 9. Influence range of seepage recharge groundwater in the secondary perched river from 2012 to 2017.

The hydraulic slope, represented by the ratio of the water head difference Δh between the water level of the secondary perched reach and the groundwater level of the wells to

the distance ΔL from the Yellow River, i.e., $\Delta h/\Delta L = J$, serves as a metric for comparing the differences in recharge between the secondary perched reach and the groundwater before and after the operation of the Xiaolangdi Reservoir. Through a comparative analysis of the long-term variation in groundwater levels across monitoring wells and the water level of the river, the groundwater hydraulic gradient was estimated to be in the range of 0.00097–0.005 on the north bank and 0.0005–0.005 on the south bank of the river.

The period 1980 to 1994 was characterized by wet conditions, with fewer human economic activities in the study area. During this time, the water quantity and water level of the Yellow River, as well as the groundwater environment on both sides of the river, primarily reflected natural conditions. The water quantity and water level of the Yellow River fluctuated greatly during this period because of hydrological conditions. Notably, monitoring wells #2, #5, #8, #9, #10, and #13, which are distributed in the western part of Henan Province, close to the Jialu River, were influenced by its water levels. Groundwater recharge at sites #8 and #9 originated mainly from the western Mangshan region. Furthermore, the correlation analysis between groundwater in the first section and the water level of the Yellow River shows that their groundwater levels (90.28 m and 99.31 m (2020)) were higher than those of the Yellow River during the same period (89.35 m). They are located in the Huaihe River Basin. When calculating the supply area from Mangshan, wells #10 and #13 were found to be closest to the Jialu River (0.6 and 0.9 km, respectively), with a higher Jialu River gradient (0.00049) but a lower gradient when calculated from the Yellow River. Wells #6, #7, and #12 were close to the south bank of the Yellow River (2.4, 6.8, and 5.4 km, respectively), which is affected by the river water level, resulting in higher gradients ($J > 0.0039$). The groundwater levels were replenished by different rivers, and the results varied. Wells #22, #23, and #24 with lower gradient values ($J < 0.00082$ – 0.00032) were closer to the eastern channel of the north bank of the Yellow River (10, 7.1, and 4.8 km, respectively). Conversely, wells #33, #34, #35, and #36 were closer to the natural Wenyan Canal to the west of the north bank of the Yellow River (0.8, 1.1, 0.5, and 1.2 km, respectively), and at distances of 17.1 km, 12.9 km, 4.6 km, and 18.3 km, respectively, from the river. The J values of 0.001, 0.0005, 0.00098, and 0.00083, reflected shorter distances from the wells to different rivers.

According to the hydraulic gradient formula, when the river and groundwater levels are in a natural state, the distance to the river is closer and the J value is higher. These low values indicate that external factors affect groundwater levels. For example, wells near river sources, farmland irrigation, and long-term groundwater exploitation result in large groundwater depression cone areas. For example, wells #37 and #38 were 1.6 km and 3.7 km away from the south bank of the Yellow River, respectively. The J value (0.00048–0.0037) varied significantly. A study revealed that the Yuanfang-Liudian Riverside Well Field in Kaifeng City, a source of river water, had been established nearby. When the water level is stable, the maximum water level in the center of the funnel drops by 15 m, significantly impacting the surrounding groundwater levels. By calculating the hydraulic slope of groundwater and considering the dynamic relationship between groundwater level and the water level of the Yellow River, regions with a significant influence of river water infiltration were determined on both sides of the river (Figure 8).

The hydraulic slope of the north bank of the Yellow River has been calculated to be greater than 0.5‰, covering an area of approximately 1800 km², while that of the south bank is approximately 1400 km² (Figure 10).

During 2012–2017, the water level of the Yellow River continued to decline from 89.29 m to 88.07 m because of the operation of Xiaolangdi Reservoir. The groundwater levels of the monitoring wells exhibited a downward trend, reaching their lowest levels in 2014 by the end of that year, the South-to-North Water Diversion channels delivered approximately 300 million m³ of water annually to Zhengzhou City and approximately 100 million m³ to Xinxiang City. In 2021, the average groundwater level had recovered to 6.46 m with a medium groundwater tapping of 1.88 m in Zhengzhou. During the water delivery period, the closure of certain pumping wells in 2015 led to a rise in groundwater

levels on both sides of the Yellow River. Influenced by various factors, such as local precipitation, industrial and agricultural consumption, and the continuous increase in urban residential water consumption, the groundwater level exhibited a gradual increase (Figure 10a,b); however, it still showed a gradual decline in 2020 (Figure 10c,d).

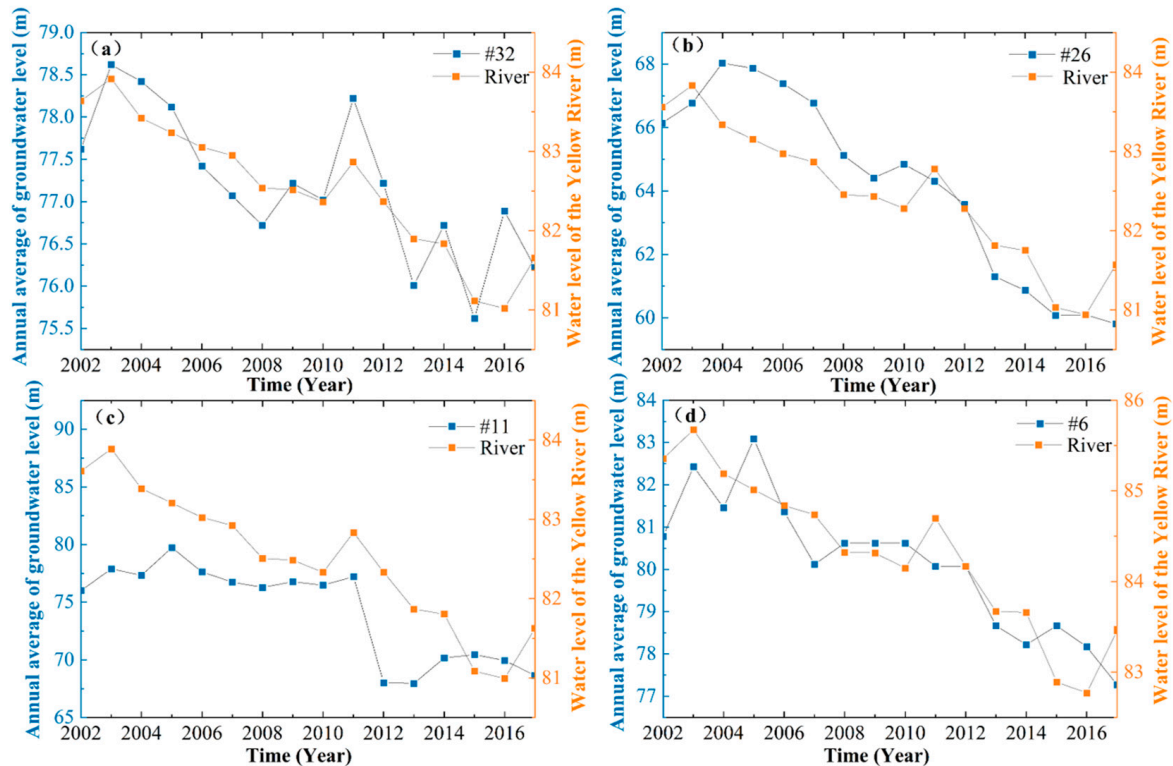


Figure 10. Relationship between the groundwater levels at various monitoring wells and the water level of the Yellow River after the operation of the Xiaolangdi Reservoir. (a) Monitoring well (#32); (b) monitoring well (#26); (c) monitoring well (#11); (d) monitoring well (#6).

During this period, the water level of the Yellow River continued to decline, and then it increased significantly after the initiation of the South-to-North Water Diversion Project in 2015 because irrigation with water from the Yellow River diversion reduced the amount of water in the receiving area, while the discharge from the Yellow River increased from Huayuankou to Jiahetan. Since 2017, at Huayuankou Station, the water level of the Yellow River has increased (from 87.94 m to 90.37 m), accompanied by an increase in discharge from 618 m³/s to 1416.3 m³/s. There was also a subsequent increase in flow (from 571 m³/s to 1370.6 m³/s) and water level (from 71.31 m to 71.99 m). As a result, the hydraulic gradient of the north bank of the Yellow River increased by 1.5‰–2‰ and that of the south bank increased by 1‰.

In terms of hydrodynamic field changes, the hydraulic slope of the northern bank of the Yellow River has increased in areas with large hydraulic slopes, especially in the monitoring wells located north of the Wenyan Canal (#30 increased from 0.00028 to 0.00043 from 2000–2010 to 2011–2020), and the extent of the large hydraulic slopes has expanded. Additionally, the hydraulic gradient of the southern bank of the river also witnessed an increase (#11 increased from 0.000082 to 0.00069 from 2000–2010 to 2011–2020) (Figure 9). The groundwater funnel areas of the four major river sources have also expanded, along with an increase in their depths. As the hydrodynamic field during this stage is influenced by various water sources, further comprehensive water source investigation and statistical analyses should be carried out.

In summary, while groundwater level distribution on both sides of the Yellow River is affected by various factors, this study primarily focused on the influence of Yellow River

infiltration on groundwater. We examined the factors that, over the past 50 years, have had the most significant impact on groundwater in this region. These factors include the formal initiation of water and sediment transfer from the Xiaolangdi Reservoir in 2002, the operation of the five major river source areas in 2010, and the initiation of the South-to-North Water Transfer Project in 2014. These events have played a crucial role in controlling Yellow River water infiltration and recharge groundwater in the Huayuankou–Jiahetan section.

4.2.2. Spatiotemporal Variation in Groundwater Recharge from the Yellow River

(1) Difference in groundwater level recharge from the Yellow River before and after reservoir operation

Owing to the differences in geological and geomorphic conditions on both sides of the Yellow River, the influence of the river water infiltration on groundwater levels yields different results. The IBM SPSS Statistics 26.0.0.0 software was used to perform single-factor ANOVA of the calculated hydraulic slope of each well. The significance of the homogeneity test of variance before and after the operation of the Xiaolangdi Reservoir was 0.799, and the significance of ANOVA was 0.000 (Table 4). For the period before the reservoir operation, spanning from 1980 to 1994 and from 1995 to 2002, the significance of the homogeneity test of variance was 0.443, and the significance of ANOVA was 0.000 (Table 5). After the reservoir operation, covering the years from 2003 to 2011 and from 2012 to 2017, the significance of the variance homogeneity test between the two banks was 0.449, and the significance of ANOVA was 0.002 (Table 6).

Table 4. Variance analysis of Xiaolangdi Reservoir before and after operation.

	Squares	Freedom	Mean Square	F	Significance
Groups	0.077	1	0.77	12.787	0.000
Interclass	0.996	166	0.006		
Total	1.073	167			

Table 5. Variance analysis of 1980–1994 and 1995–2002.

	Squares	Freedom	Mean Square	F	Significance
Groups	0.110	1	0.11	25.985	0.000
Interclass	0.348	82	0.004		
Total	0.458	83			

Table 6. Variance analysis of 2003–2011 and 2012–2017.

	Squares	Freedom	Mean Square	F	Significance
Groups	0.062	1	0.062	10.678	0.002
Interclass	0.474	82	0.006		
Total	0.535	83			

(2) Difference in groundwater level recharge on both sides of the secondary perched river before and after operation of the Xiaolangdi Reservoir

Before and after operation of the reservoir, the significance of the homogeneity test of variance between the south and north banks was 0.191 and the significance of ANOVA was 0.000 (Table 7). Before operation, the significance of the variance homogeneity test was 0.565 and that of ANOVA was 0.027 (Table 8). After operation, the significance of the homogeneity test of variance between the northern and southern banks was 0.38 and the significance of ANOVA was 0.000 (Table 9).

Table 7. Variance analysis of the south bank and north bank before and after operation.

	Squares	Freedom	Mean Square	F	Significance
Groups	0.111	1	0.111	19.079	0.000
Interclass	0.962	166	0.006		
Total	1.073	167			

Table 8. Variance analysis of the south bank and north bank before operation.

	Squares	Freedom	Mean Square	F	Significance
Groups	0.027	1	0.27	5.068	0.027
Interclass	0.433	82	0.005		
Total	0.46	83			

Table 9. Variance analysis of the south bank and north bank after operation.

	Squares	Freedom	Mean Square	F	Significance
Groups	0.094	1	0.94	17.452	0.000
Interclass	0.442	82	0.005		
Total	0.536	83			

5. Discussion

5.1. Response of Groundwater to Water Level Changes in the Yellow River after Operation of the Xiaolangdi Reservoir

Before the operation of the Xiaolangdi Reservoir, from 1972 to 1998, the variations in the water levels within the Huayuankou and Jiahetan sections of the Yellow River were 90.82 to 91.48 m (a decrease of 0.66 m) and 82.0 to 75.84 m (a decrease of 6.16 m), respectively, reflecting a stable natural state (Table 10). During this period, the water table also maintained a natural state. Using dynamic methods, it was difficult to establish a clear relationship between the Yellow River water levels in both affected and non-affected regions, unless significant disparities existed in groundwater level dynamics between the two regions. After reservoir operation, owing to the annual transfer of water and sediment, the minimum discharge in the flat bed of the channel within the reach increased from 620 m³/s before the 2002 flood to 1040 m³/s in 2013. With continuous scouring, the riverbed of the lower Yellow River continues to become coarser, with the median particle size of bed sand, D₅₀, generally increasing by 1–2 times [17]. This leads to an approximately two-fold increase in the formation permeability coefficient ($K = d_x^2$, where d is the particle size of the gradation x), which is conducive to the infiltration of the river water to recharge groundwater. The erosion and scouring of the riverbed by the river have resulted in an evident drop in the river level between the Huayuankou and Jiahetan hydrological stations [36]. However, owing to the reduced river level, the gradient between the river level and groundwater level has reduced, affecting the intensity of river water infiltration. Therefore, the combined effect of changes in riverbed grain size and decreased river levels on groundwater have represented a challenge following the operation of the reservoir. Further investigation through field tests and research is required to better understand this phenomenon. A significant decrease in the water level of the Yellow River leads to a corresponding decline in the groundwater level of the riverbank within the river-affected area. The degree of this decline depends on the synchronicity of these two changes, determining the extent to which the groundwater level is affected by the river level. For example, the distances between wells #3, #6, #31, #32, #33, #35, #26, and #45 on both sides of the Yellow River vary, indicating differences in how intensely the groundwater level is affected by changes in the water level of the river. Monitoring wells located near the river (#31, #32, #33, and #26) showed a continuous decline in water level over five years, whereas those located far from the river showed a downward trend in the second or third

year (#3 and #35). In contrast, the water level of monitoring well #45 remained unaffected by changes in the Yellow River's water level and showed no downward trend.

Table 10. Groundwater level dynamics of some monitoring wells after the operation of the Xiaolangdi Reservoir.

Time	Water Level of Huayuankou	Water Level of Jiahetan	#3 (15.85)	#6 (2.35)	#31 (0.62)	#32 (5.82)	#33 (17.02)	#35 (4.86)	#26 (25.71)	#45 (21.29)
2000	91.32	76.01	74.02	66.09	78.61	77.97	73.53	86.04	68.12	62.31
2001	90.84	75.72	73.56	67.38	79.34	77.83	73.52	86.41	67.95	62.19
2002	90.62	74.54	73.10	67.72	77.19	77.77	71.85	86.18	66.43	62.95
2003	90.55	74.44	73.42	66.09	76.98	77.86	71.19	85.60	66.09	62.79
2004	90.16	73.89	73.95	67.385	77.12	77.87	72.59	85.84	67.38	63.13
2005	90.01	73.64	74.13	67.72	77.61	78.00	72.78	85.45	67.72	61.75

Note: Water level (m) is the annual average water level, and the distance from the Yellow River is shown in km below the monitoring well number, e.g., (2.35).

In summary, the operation of the Xiaolangdi Reservoir has led to a significant decrease in the river level. Over the past two decades, the river level at Huayuankou Station has decreased by 1.97 m and that at Jiahetan Station by 4.17 m. Simultaneously, the groundwater level has also decreased. For instance, well #31, located adjacent to the levee on the north bank of the Yellow River at a distance of 0.62 km from the river, has experienced a decrease of 3.12 m in groundwater level. Well #32, located 5.82 km away from the riverside, has witnessed a groundwater level decrease of 3.82 m. On the south bank, well 6, located 2.35 km away from the river, has experienced a groundwater level drop of 5.19 m. Meanwhile, well #11, situated 12.14 km away from the river, has recorded a significant groundwater level decline of 10.21 m.

5.2. Influence of Riverside Well Fields along the Yellow River on Groundwater Levels

Since 2000, five large Riverside Well Fields have been constructed along both sides of the Yellow River. Presently, the depth of groundwater level decline has reached an average of 25 m. The water source mining well group was located 1 km from the riverside, particularly in the Zhengzhou ($15 \times 10^4 \text{ m}^3/\text{d}$) and Kaifeng Riverside Well Fields ($20 \times 10^4 \text{ m}^3/\text{d}$). Currently, the decline in the water table has extended to 50–70 m along the Yellow River. As of 2020, the center of the west Zhengzhou groundwater depression cone was located in Guying Town, Xingyang City, with a groundwater level of 42–46 m and an elevation of 61.58 m. The center of the eastern depression cone encompasses the outer ring of Longzi Lake and the area of Zhongmu Pingan Avenue, with a groundwater level of 17–20 m and an elevation of 66.56 m.

The groundwater depression cones (#29 and #20) of the Yuanyang and Fengqiu water sources were approximately 1 km away from the boundary line of the Yellow River, with the groundwater level at 17–18 m. The center of the groundwater depression cone of the Kaifeng water source was 1.65 km away from the boundary line of the river, with a depth of 15 m.

It is evident that local groundwater depression cone areas have formed in each river source area, distributed on both sides of the Yellow River and forming a local catchment area at the center of the groundwater depression cone. As the hydraulic slope increases, the infiltration of river water increases the intensity of the shallow groundwater. Within the distribution area of a groundwater depression cone, the area closest to the influence zone of the Yellow River water recharge should be defined at the southern boundary of the groundwater depression cone. Therefore, in the distribution area of the groundwater depression cone, the influence zone of the river water recharge should be defined at the center of the cone (Figure 9, Table 11). Hence, the farthest influence distance of Yellow River water infiltration for recharging groundwater in the Zhengzhou–Zhongmou area on the south bank was 22.6 km, which was similar to the farthest influence distance of river water infiltration for recharging groundwater when there is no river source area. The maximum distance of influence of the unsealed funnel region was 7 km. The farthest

influence distance outside the descending funnel zone of Zhandian–Yuanyang on the north shore was 1.5 km, and the farthest influence distance outside the descending funnel zone of Fengqiu–Jinglonggong was 1 km. The groundwater level of other water sources decreased less, except for the water source for Zhengzhou City, where extensive mining has led to a significant drop in groundwater levels, resulting in a large groundwater depression cone area that was distant from the Yellow River recharge.

Table 11. Falling funnel of the river source area in the Huayuankou–Jiahetan section.

Name of Water Source	GDC Area (km ²)	GDC Depth (m)	Distance between the Back Side of the GDC and Yellow River (km)	Shallow Groundwater Exploitation Quantity (10 ⁴ m ³ /d)	Distance between and Yellow River (m)
Yuanyang County Yuanwu–Baochang water source	302	18	19.6	35	1000
Dongzhang–Langchenggang water source area, Zhongmu County	216	12	16.6	15	1000
Yuanfang–Liudian water source, Kaifeng County	200	15	16.0	20	1000
Zhandian water source in Wuzhi County	125	5	12.6	15	1000
Jinglonggong water source of Fengqiu County	61	17	8.8	10	1000
The northern suburbs of Zhengzhou City and the ‘Ninth Five-Year’ water source area	>400	20	22.6	15	7500

Note: Some of the data were drawn from Zhengzhou and Xinxiang 2020/2021 Water Resources Bulletins; GDC—groundwater depression cone.

The fact is that the water resources in the secondary perched reaches of the Yellow River have a vital impact on the economic development, the production and life of the residents, and the ecological environment in the lower reaches of the Yellow River. At present, due to the economic development and population increase in this area, the exploitation of river water and groundwater has increased greatly, resulting in the reduction of river flow and the decrease of river water level and groundwater levels in the studied section. At present, due to the economic development and population increase in this area, the exploitation of river water and groundwater has increased greatly, resulting in the reduction of river flow and the decrease of river water level and groundwater levels in the studied section. Especially in the water source area along the riverbank, groundwater drop funnels appear in many places, and most of the ecological wetlands shrink or disappear. The operation of Xiaolangdi Reservoir and the South-to-North Water Diversion channel result in water resources being injected into the secondary perched reaches section, which alleviates the water demand in this area to a large extent. However, the change in the natural conditions of the river and the impact on the water quality and ecological environment caused by the intensified infiltration of groundwater are also gradually prominent. In order to reduce the impact of man-made projects on economic development, residents’ lives, and the ecological environment, it is necessary to carry out the following studies:

1. Carry out in-depth basic research on the interaction between river water and groundwater in the region.
2. Investigate and study the quality of surface water and groundwater, especially the pollution of groundwater by surface polluted water.
3. Implement the joint deployment of surface water and groundwater and carry out research on the comprehensive utilization of water resources in large regions (or river basins).
4. Formulate plans for rational development, utilization, and conservation of water resources to provide a scientific basis for ensuring sustainable economic development and protecting the ecological environment.

6. Conclusions

1. Before and after the operation of the Xiaolangdi Reservoir, the significance of the one-way ANOVA was 0.000, which is less than 0.05, indicating differences in the infiltration and recharge of river water to groundwater. Similarly, the significance of the one-way ANOVA between the south and north banks of the Yellow River was 0.000, which is also less than 0.05, suggesting differences in groundwater recharge between the two banks.
2. The shallow groundwater dynamic field on both sides of the Yellow River is primarily controlled by paleogeomorphology and stratigraphic lithology. In areas with ancient rupture fans and ancient channels, the hydraulic gradient is generally larger, ranging from 2‰ to −5‰. After the operation of Xiaolangdi Reservoir, the influence range of the secondary perched reach on the southern bank of the Yellow River increased from 15.85–16.13 km to 18.43–21.05 km. Similarly, on the northern bank, the influence range increased from 20.13–20.48 km to 23.41–26.74 km.
3. The five large Riverside Well Fields established on both sides of the Yellow River within the study area have been in operation for more than two decades. Currently, they have extracted a total of 1×10^6 m³/d of groundwater, resulting in the formation of several groundwater depression cones within their operational range. The groundwater level in the center of these shallow groundwater depression cones has decreased by 20–42 m in the Jiuwu and Beijiao water sources of Zhengzhou and by 17–18 m in other water sources. The formation of these groundwater depression cones along the banks of the Yellow River has altered the hydrodynamic field of the shallow groundwater in these areas and has weakened the infiltration and recharge of the river water to the shallow groundwater.
4. The groundwater recharge in the Huayuankou–Jiahetan secondary perched reach is affected by numerous factors. This section experiences a multitude of large-scale human activities, including the Yellow River diversion irrigation project, canal leakage, mechanized wells for agricultural irrigation, and domestic water supply. These activities often interfere with each other, leading to irregular changes in groundwater levels. For instance, in some monitoring wells (#3, #10, #34, #43, and #45), the fluctuations in groundwater levels lagged behind those of the Yellow River by 2–3 years or longer. Additionally, many monitoring wells were sensitive to the South-to-North Water Transfer Project, which began in 2014. However, in some wells (#16, #18, #28, and #30), the groundwater levels did not significantly reflect any human activities in the area, making them worthy subjects for further study.

Author Contributions: Conceptualization, M.Z. and J.P.; methodology, Y.Z.; software, H.L.; formal analysis, J.M.; investigation, J.Z.; resources, J.L.; All authors have read and agreed to the published version of the manuscript.

Funding: This research was funded by the Research Startup Fund for the Academician Team of Zhengzhou University (Grant No. 13432340370), the high-level talents of Zhengzhou University (Grant No. 134-32340364 and No. 135-32340122), and the National Natural Science Foundation of China–Henan Talent Training Joint Foundation (Grant No. U1504404).

Data Availability Statement: Data included in the article.

Acknowledgments: Special thanks are given for the water level and flow data of Huayuankou and Jiahetan Hydrological Stations in the lower reaches of the Yellow River from 1980 to 2017 provided by the Yellow River Water Conservancy Commission. Special thanks are given to the Henan Provincial Bureau of Hydrology and Water Resources to for providing ‘Henan groundwater data’.

Conflicts of Interest: The authors declare no conflict of interest.

References

1. Lu, M.W.; Zhao, Q.H.; Ding, S.Y.; Lu, X.L.; Jing, Y.R.; Wang, S.Q.; Hong, Z.D.; Wang, A. Lag response of groundwater to changes in water and sediment characteristics in the lower yellow river, china. *J. Hydrol.* **2022**, *612*, 128048. [[CrossRef](#)]

2. Zhao, Y.Z.; Shao, J.L.; Jiao, H.J.; Yan, Z.P. Basic characteristics of groundwater reservoirs of the affected zone along the Lower Yellow River in Henan Province. *J. Hydraul. Eng.* **2003**, *4*, 90–93, 100.
3. Bruwier, M.; Erpicum, S.; Piroton, M.; Archambeau, P.; Dewals, B.J. Assessing the operation rules of a reservoir system based on a detailed modelling chain. *Nat. Hazards Earth Syst. Sci.* **2015**, *15*, 365–379. [[CrossRef](#)]
4. Javadzadeh, H.; Ataie-Ashtiani, B.; Hosseini, S.M.; Simmons, C.T. Interaction of lake-groundwater levels using cross-correlation analysis: A case study of Lake Urmia Basin, Iran. *Sci. Total Environ.* **2020**, *729*, 138822. [[CrossRef](#)] [[PubMed](#)]
5. Ali, G.A.; L'Heureux, C.; Roy, A.G.; Turmel, M.; Courchesne, F. Linking spatial patterns of perched groundwater storage and stormflow generation processes in a headwater forested catchment. *Hydrol. Process.* **2011**, *25*, 3843–3857. [[CrossRef](#)]
6. Beetle-Moorcroft, F.; Shanafield, M.; Singha, K. Exploring conceptual models of infiltration and groundwater recharge on an intermittent river: The role of geologic controls. *J. Hydrol. Reg. Stud.* **2021**, *35*, 100814. [[CrossRef](#)]
7. Chen, J.G.; Zhou, W.H.; Sun, P. Effects of water-sediment regulation by Xiaolangdi Reservoir on channel erosion in the Lower Yellow River. *J. Sedim. Res.* **2009**, *34*, 1–7.
8. Salve, R.; Rempe, D.M.; Dietrich, W.E. Rain, rock moisture dynamics, and the rapid response of perched groundwater in weathered, fractured argillite underlying a steep hillslope. *Water Resour. Res.* **2012**, *48*. [[CrossRef](#)]
9. Shang, H.X.; Sun, Z.Y.; Tian, S. Scouring and Siltation Characteristics in the Lower Yellow River Since 2000. *Yellow River* **2015**, *37*, 7–12.
10. Li, X.P.; Liu, X.Y.; Li, Y. Study on Erosion and Deposition Trend in the Future in the Lower Yellow River. *Yellow River* **2016**, *38*, 1–3.
11. Sun, Z.Y.; Shang, H.X.; Peng, H. Analysis on the Discharging Capability of the Lower Yellow River Channel during 2018 Flood Season. *Yellow River* **2019**, *41*, 8–12.
12. Zhang, F.X.; Shi, Y.P.; Bi, G.Z.; Wang, M. Study on the Law of the Channel Scouring and Siltation under Different Treatment Scheme in Lower Yellow River. *Yellow River* **2019**, *41*, 36–43.
13. Currie, D.; Laattoe, T.; Walker, G.; Woods, J.; Smith, T.; Bushaway, K. Modelling Groundwater Returns to Streams from Irrigation Areas with Perched Water Tables. *Water* **2020**, *12*, 956. [[CrossRef](#)]
14. Su, C.; Zhang, X.Q.; Fei, Y.H.; Li, Z.; Meng, S.H.; Cui, X.X.; Pan, D.; Yang, P.J.; Guo, C.Y.; Tian, X. Lateral seepage scope of downstream of Yellow River after the operation of Xiaolangdi reservoir and its impact on groundwater environment. *Geol. China* **2021**, *48*, 1669–1680.
15. Yang, D.; Li, C.; Hu, H.; Lei, Z.; Yang, S.; Kususa, T.; Koike, T.; Musiaka, K. Analysis of water resources variability in the Yellow river of china during the last half century using historical data. *Water Resour. Res.* **2004**, *40*, W06502. [[CrossRef](#)]
16. Ji, H.; Chen, S.; Jiang, C.; Fan, Y.; Fu, Y.; Li, P.; Liu, F. Damming-Induced Hydrogeomorphic Transition in Downstream Channel and Delta: A Case Study of the Yellow River, China. *Water* **2022**, *14*, 2079. [[CrossRef](#)]
17. Shen, G.Q.; Li, Y.; Zhang, Y.F.; Peng, H. Sediment Trapping by Xiaolangdi Reservoir on Deposits Reduction in the Lower Yellow River. *Yellow River* **2020**, *42*, 1–6.
18. Yu, Y.; Xia, J.Q.; Li, J.; Zhang, X.L. Influences of the Xiaolangdi Reservoir on the channel geometry and flow capacity of wandering reach in the Lower Yellow River. *J. Sediment Res.* **2020**, *45*, 7–15.
19. Liu, W.; Wang, S.; Sang, Y.; Ran, L.; Ma, Y. Effects of large upstream reservoir operations on cross-sectional changes in the channel of the lower Yellow River reach. *Geomorphology* **2021**, *387*, 107768. [[CrossRef](#)]
20. Liang, H.T.; Lyu, H.; Wang, W.K.; Bai, J.; Wang, J.M.; Yan, Y.M.; Dong, W.H.; Su, X.S. Seasonal scour and siltation induced spatiotemporal variations in riverbed sediment leakage coefficients as measured via the thermal tracer method. *J. Hydrol.* **2023**, *626*, 130136. [[CrossRef](#)]
21. Ni, C.-F.; Tran, Q.-D.; Lee, I.-H.; Truong, M.-H.; Hsu, S.M. Mapping Interflow Potential and the Validation of Index-Overlay Weightings by Using Coupled Surface Water and Groundwater Flow Model. *Water* **2021**, *13*, 2452. [[CrossRef](#)]
22. Sun, L.; Wang, L.L.; Cao, W.G. Evolution of Groundwater Hydrochemical Characteristics in the Influence Zone of the Lower Yellow River in Henan. *Yellow River* **2021**, *43*, 91–99.
23. Li, X.; Yan, B.; Wang, Y.; Wang, X.; Li, Y.; Gai, J. Study of the Interaction between Yellow River Water and Groundwater in Henan Province, China. *Sustainability* **2022**, *14*, 8301. [[CrossRef](#)]
24. Germer, S. Development of near-surface perched water tables during natural and artificial stemflow generation by babassu palms. *J. Hydrol.* **2013**, *507*, 262–272. [[CrossRef](#)]
25. Lu, M.; Zhao, Q.; Ding, S.; Wang, S.; Hong, Z.; Jing, Y.; Wang, A. Hydro-geomorphological characteristics in response to the water-sediment regulation scheme of the Xiaolangdi Dam in the lower Yellow River. *J. Clean. Prod.* **2022**, *335*, 130324. [[CrossRef](#)]
26. Hong, Z.D.; Ding, S.Y.; Zhao, Q.H.; Geng, Z.H.; Qiu, P.W.; Zhang, J.; Wang, A.; Zhang, P.P. Relative contribution of multi-source water recharge to riparian wetlands along the lower Yellow River. *J. Environ. Manage.* **2022**, *321*, 115804. [[CrossRef](#)]
27. Balvín, A.; Hokr, M.; Šteklová, K.; Rálek, P. Inverse modeling of natural tracer transport in a granite massif with lumped-parameter and physically based models: Case study of a tunnel in Czechia. *Hydrogeol. J.* **2021**, *29*, 2633–2654. [[CrossRef](#)]
28. Han, Y.; Bu, H. The impact of climate change on the water quality of Baiyangdian Lake (China) in the past 30 years (1991–2020). *Sci. Total Environ.* **2023**, *870*, 161957. [[CrossRef](#)]
29. Zhao, L.; Zhang, Z.; Dong, F.; Fu, Y.; Hou, L.; Liu, J.; Wang, Y. Research on the Features of Rainfall Regime and Its Influence on Surface Runoff and Soil Erosion in the Small Watershed, the Lower Yellow River. *Water* **2023**, *15*, 2651. [[CrossRef](#)]
30. Kumar, G.S. Mathematical Modeling of Groundwater Flow and Solute Transport in Saturated Fractured Rock Using a Dual-Porosity Approach. *J. Hydrol. Eng.* **2014**, *19*, 986.

31. Wendland, E.; Gomes, L.H.; Troeger, U. Recharge contribution to the Guarani Aquifer System estimated from the water balance method in a representative watershed. *An. Acad. Bras. Cienc.* **2015**, *87*, 595–609. [[CrossRef](#)] [[PubMed](#)]
32. Sajil Kumar, P.J.; Schneider, M.; Elango, L. The State-of-the-Art Estimation of Groundwater Recharge and Water Balance with a Special Emphasis on India: A Critical Review. *Sustainability* **2022**, *14*, 340. [[CrossRef](#)]
33. Tao, Y.Z.; Xi, D.Y. Rule of transient phreatic flow subjected to vertical and horizontal seepage. *Appl. Math. Mech. (Engl. Ed.)* **2006**, *27*, 59–65. [[CrossRef](#)]
34. GB/T 22482-2008; Standard for Hydrological Information and Hydrological Forecasting. National Standard: Beijing, China, 2009.
35. Rahmati, M.; Vanderborght, J.; Simunek, J.; Vrugt, J.A.; Moret-Fernandez, D.; Latorre, B.; Lassabatere, L.; Vereecken, H. Soil hydraulic properties estimation from one-dimensional infiltration experiments using characteristic time concept. *Vadose Zone J.* **2020**, *19*, e20068. [[CrossRef](#)]
36. Zhang, X.; Qiao, W.; Lu, Y.; Huang, J.; Xiao, Y. Quantitative Analysis of the Influence of the Xiaolangdi Reservoir on Water and Sediment in the Middle and Lower Reaches of the Yellow River. *Int. J. Environ. Res. Public Health* **2023**, *20*, 4351. [[CrossRef](#)]

Disclaimer/Publisher’s Note: The statements, opinions and data contained in all publications are solely those of the individual author(s) and contributor(s) and not of MDPI and/or the editor(s). MDPI and/or the editor(s) disclaim responsibility for any injury to people or property resulting from any ideas, methods, instructions or products referred to in the content.